Single-Molecule Studies of Sol–Gel-Derived Silicate Films. Microenvironments and Film-Drying Conditions

ARTICLE *in* THE JOURNAL OF PHYSICAL CHEMISTRY B · OCTOBER 2000

Impact Factor: 3.3 · DOI: 10.1021/jp001011h

4 AUTHORS, INCLUDING:

Maryanne M Collinson
Virginia Commonwealth University
94 PUBLICATIONS **3,155** CITATIONS

SEE PROFILE

Single-Molecule Studies of Sol−Gel-Derived Silicate Films. Microenvironments and Film-Drying Conditions

Erwen Mei,† Angela M. Bardo, Maryanne M. Collinson,* and Daniel A. Higgins*

Department of Chemistry, Kansas State University, Manhattan, Kansas 66506-3701

Received: March 16, 2000; In Final Form: September 4, 2000

Single-molecule spectroscopy is used to characterize the microenvironments found in silicate thin films dried under different conditions. Local film properties are assigned on the basis of the fluorescence emission characteristics of individual dopant (rhodamine B) molecules. The samples studied include those characterized immediately after being spin cast onto a glass substrate (fresh samples) and after drying at ≈80 °C in a vacuum oven for at least 12 h (dried samples). The single-molecule fluorescence spectra shift to the red for films dried under more rigorous conditions, reflecting increased average film polarity. The distribution of fluorescence emission maxima also broadens slightly with drying, reflecting an increase in film heterogeneity. Bimodal distributions in the widths of the emission maxima are observed. These distributions exhibit a narrowing of the single-molecule emission with drying, pointing to greater microenvironmental rigidity. Studies of the time-dependent emission characteristics of the single molecules show the total number of photons emitted (prior to bleaching) by the molecules in the dried films is four (3.6 ± 0.6) times greater than in the fresh films. A 4-fold (4.3 ± 0.7) increase in the average survival time of the molecules is also observed, proving that increased dye emission from the dried films results primarily from an increase in dye stability, rather than an increase in fluorescence quantum yield. It is also shown that the single-molecule emission fluctuates more rapidly in the dried films, possibly due to an increase in the rate of triplet formation and/or an increase in the triplet lifetime. Increased dopant stability is attributed to reduced oxygen and dye mobility within the more dense, highly cross-linked silicate network of the dried films. FTIR studies of the thin films provide additional support for these conclusions.

I. Introduction

Sol−gel technology[1] has been used to prepare inorganic and organic−inorganic composite films through the hydrolysis and condensation of metal alkoxides, most notably the silicon alkoxides (i.e., tetramethoxysilane).[2−5] These materials are now being developed for use in chemical sensors and other photonic and solid-state devices.[6−12] Many of these applications utilize the spectroscopic and/or electrochemical response of reagents entrapped within the solid silicate hosts.[2−9] Previous work has established that these entrapped reagents retain their solution-phase chemical and physical properties and are accessible to external species via diffusion through the porous silicate network.[2,3,5,13] Chelating agents, indicator dyes, proteins, enzymes, antibodies, zeolites, cyclodextrins, and crown ethers are examples of the many different types of reagents that have been trapped within the silica framework.[2−9]

Of utmost importance in many applications of sol−gel-derived materials is the nature of reagent entrapment.[3,5] Device performance is strongly influenced by the translational and rotational mobility of entrapped species, the degree and chemical nature of molecular interactions with the walls of the matrix, and the molecular scale properties (polarity, rigidity) of the individual cages/pores in the host framework. As a result, numerous bulk spectroscopic, electrochemical, and chemical studies have been performed.[6,7,14−25] These previous studies have provided valuable information on the average chemical environment surrounding entrapped reagents. However, very few sites within these materials actually possess the average properties.[7,15,16,26] A complete understanding of their properties can only be obtained from additional studies that allow for the full distribution of environments to be characterized.

In previous work we have shown that single-molecule imaging[27,28] and spectroscopy[28−30] can provide valuable new information about the microheterogeneity of dye doped silicate films.[31] Using rhodamine B (RhB) as the photophysical probe, these studies have shown that silicate films are considerably more heterogeneous than organic polymer films prepared from poly(butyl methacrylate). The distribution of single-molecule fluorescence emission maxima in the silicate was shown to be much broader than in the organic polymer. In addition, the spectrally integrated, time-dependent emission (fluorescence transients) from individual molecules was shown to be similarly sensitive to the local environment. Significantly more fluctuations were observed in the fluorescence transients from the silicate-entrapped molecules. Importantly, these results also showed a much broader range of behaviors in the silicate films, pointing to greater material heterogeneity.

In this work, these studies are extended to better understand the effects of varied preparation conditions and film chemical composition (i.e., solvent content) on the properties of molecular-scale environments within silicate thin films. Specifically, the dependence of film properties on the extent of film drying is explored via a detailed analysis of the fluorescence spectra and signal fluctuations of gel-entrapped RhB molecules. These results show that rigorously dried films are more heterogeneous

* Author to whom correspondence should be addressed.
† Present address: Department of Chemistry, University of Pennsylvania, Philadelphia, PA.

10.1021/jp001011h CCC: $19.00
Published on Web 10/10/2000

than corresponding freshly prepared films. In addition, dopant molecules entrapped in dried films are found to be approximately four times more stable than their fresh-film counterparts, emitting four times more photons on average, prior to photobleaching.

II. Materials and Methods

A. Samples. Silicate films were prepared by mixing tetramethoxysilane (TMOS, Aldrich, 98%), methanol (spectrophotometric grade), deionized water, and 0.1 M HCl in a mole ratio of 1:8:7:0.003 to form the sol. The deionized water was Type I and was purified in a LabConco 4-cartridge system. The sol was allowed to stand for ≈48 h, after which Rhodamine B (RhB, Aldrich) was added to yield a concentration of 3 nM. Thin films of the dye-doped sols were then spin cast (at 6000 rpm) onto microscope cover slips (Fisher) that had been cleaned by sequential sonication in KOH, H_2SO_4, and deionized water, and dried under N_2. For the FTIR studies (see below), the films were prepared in a similar manner, using silicon substrates.

Three different film-drying procedures were employed. In one set of samples, the silicate films were cast onto substrates 30 min after addition of the dye to the sol. These films were immediately transferred to the microscope for characterization and are referred to as "fresh samples" below. A second class of samples was produced by drying the spin cast films for at least 12 h under vacuum (≈150 mTorr) at room temperature. The final set of samples were dried for at least 12 h under vacuum at ≈80 °C. These films are referred to below as "dried samples". To prevent introduction of fluorescent impurities in the vacuum-drying procedures, all samples were dried in a rigorously cleaned glass bell jar. No detectable increase in the background fluorescence from undoped control samples was observed under these conditions.

B. Instrumentation. A sample-scanning confocal microscope was employed here and has been described previously.[31] Briefly, the sample-scanning stage (Queensgate) employs closed-loop X,Y feedback for accurate sample positioning and location of individual molecules. The sample and stage were mounted on an inverted, epi-illumination microscope (Nikon). The 514.5 nm line of an argon ion laser and the 543.5 nm line from a HeNe laser were used in separate experiments to excite the dye molecules. The power at the sample in each case was maintained in the 100 nW−1.5 μW range, depending on the experiment (see below). A 10×, 1.3 numerical aperture objective was used to produce a nearly diffraction-limited focus of ≈300 nm diameter on the sample. The same objective was used to collect the fluorescence emitted by the molecules. Appropriate notch (Kaiser Optical) and band-pass filters (Omega) were used to spectrally isolate the collected fluorescence. A single-photon counting avalanche diode, positioned in a secondary image plane of the microscope, was used to detect the fluorescence in imaging experiments.

Detailed information on the nature of the silicate film microenvironments was obtained from single-molecule fluorescence spectra and from experiments in which the spectrally integrated single-molecule fluorescence was recorded in time (referred to here as "fluorescence transients"). These latter experiments were used to observe and characterize time-dependent fluctuations in the single-molecule emission rate. In both experiments, the molecules were first located by recording a fluorescence image of a 5 × 5 μm area (see Figure 1). Individual molecules were then positioned (one at a time) within the focal volume of the microscope. Fluorescence spectra were recorded using an imaging spectrograph (Acton Research) and

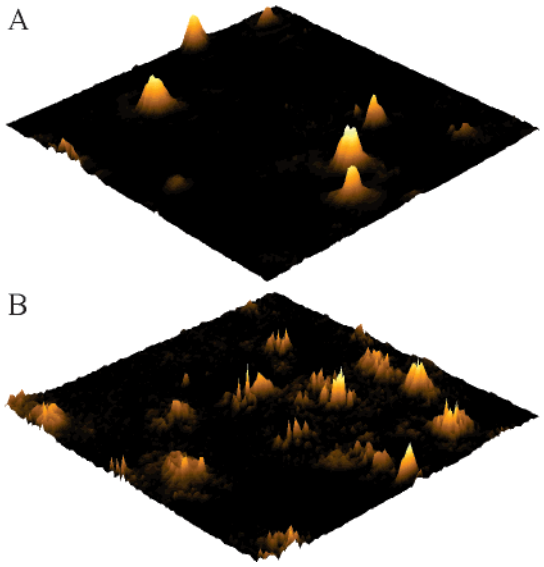

Figure 1. (A) Typical fluorescence image recorded for silicate films characterized immediately after preparation. The maximum fluorescence and background counts in this image are 1681 and 19 ± 9 counts, respectively. (B) Typical image recorded for silicate films characterized after drying for a minimum of 12 h at ≈80 °C under vacuum. The contrast has been enhanced in (B) in order to better depict the signal fluctuations observed for single molecules in the dried sample. The maximum fluorescence and background counts are 212 and 11 ± 4 counts, respectively. Both images are of 5 × 5 μm areas.

associated liquid-N_2-cooled CCD array detector (Princeton Instruments). Fluorescence transients were obtained by recording the fluorescence from each molecule until a discrete photobleaching transition was observed. These signals were recorded with time resolutions of 0.5, 2, and 10 ms. Incident powers were set to 1.5 μW, 400 nW, and 200 nW, respectively, in these experiments. Incident powers of 100, 200, and 400 nW were used in studies verifying the power dependence of signal fluctuations in the fluorescence transients. The contributions of spectral diffusion[32,33] to the signal fluctuations were assessed by recording series of single-molecule fluorescence spectra (50) with 0.5 s time resolution.

Fourier transform infrared absorption spectra were recorded in transmission mode using a Nicolet Nexus 670 spectrometer. The spectra (average of 32 scans) were recorded from 4000 to 400 cm^{-1} at a resolution of 4 cm^{-1}. A clean silicon wafer was used for recording background spectra.

III. Results

Typical fluorescence images recorded for fresh and dried samples are shown in Figure 1. The observed fluorescent spots are attributed to emission from single RhB molecules, as verified by a number of well-established arguments.[27] While such images are used primarily for locating the molecules, they also provide important initial clues as to differences between films dried under different conditions. Most notably, the image of the fresh sample (Figure 1A) shows bright, well-defined fluorescence spots, while the image of the dried sample (Figure 1B) shows the single-molecule emission to be more "noisy". The "noisy" appearance of this image results from increased fluctuations in the single-molecule emission. These fluctuations occur between several nonzero signal levels and also between nonzero levels and the background (see below). The time scales on which some of these fluctuations occur is similar to the image pixel time (40 ms). Such phenomena have been observed previously for different samples,[34−37] and for RhB-doped silicate films.[31] The

discrete "blinking transitions" to and from the background level are likely due to intersystem crossing to a triplet excited state.[35] Consistent with this mechanism, power-dependent studies (see below) show the signal fluctuation rate increases monotonically with an increase in power for the vast majority of single molecules studied. However, the exact origins of the other signal fluctuations (i.e., spectral diffusion)[32,33] are at present unknown. Despite uncertainties in their origin, it is now clear that blinking and other signal fluctuations are highly sensitive to the properties of the local molecular-scale environment.[31,37]

The fluorescence spectra for numerous individual molecules have been recorded to determine how the polarity and rigidity of the microenvironments in which the single molecules are entrapped vary with film-drying conditions. These data also provide valuable information on the spatial variations of these properties within individual films, thereby providing an important measure of film heterogeneity. For this analysis, the fluorescence spectra were fit to Gaussian functions. Their maxima and widths (full width at half-maximum, fwhm) were then tabulated. The precision of values obtained from these fits is ± 0.5 nm for the emission maximum and ± 50 cm^{-1} for the fwhm. The data for the fresh and dried samples are presented in Figure 2 in the form of histograms. The histograms have been fit to Gaussian functions to obtain quantitative information of the peak positions and widths of the distributions. Shown in these data are small, yet significant, differences in the average emission characteristics for the two samples. The fresh sample emission maximum is centered at 564.8 ± 0.5 and the dry sample at 568.7 ± 0.5 nm, giving an average red shift of 4 ± 0.5 nm for the dry sample. In addition, the distribution of emission maxima is slightly broader for the dried samples. A fwhm of 14 ± 1 nm is found for the dried sample, compared to 13 ± 1 nm for the fresh sample. In a previous paper,[31] we have shown that these distributions are approximately a factor of 2 broader than is observed for RhB-doped films of organic polymer, indicative of the greater heterogeneity of the silicate films.

The spectral width data presented in Figure 2 also reflect slight differences in the properties of the fresh and dried films. Two Gaussian functions were used to fit the width histograms. A subtle shift to smaller values for the maxima of the width distributions is observed for the dried samples. The distributions are centered at 853 ± 6 cm^{-1} and 1100 ± 25 cm^{-1} for the dried film data and at 900 ± 6 cm^{-1} and 1200 ± 25 cm^{-1} for the fresh films. The distribution widths are similar for the two samples. Samples dried under intermediate conditions (under vacuum, at room temperature) yield results that fall between those given in Figure 2.

Further important clues as to the chemical/physical microenvironmental properties of the silicate films were obtained by recording and analyzing fluorescence transients from several hundred RhB molecules in the silicate films. Figure 3A presents a fluorescence transient (10 ms resolution) representative of those observed from single molecules in dried films. In the trace shown, a shutter blocking the laser light was opened just less than 1 s after the trace was initiated. The molecule photobleached after approximately 19 s of continuous illumination, as deduced by the discrete drop in emission to the background level. During the time prior to photobleaching, the molecule was observed to exhibit significant (greater than expected for shot noise) signal fluctuations (i.e., blinking and fluctuations between nonzero levels).

The individual fluorescence transients were analyzed using a number of procedures. First, the total number of photons

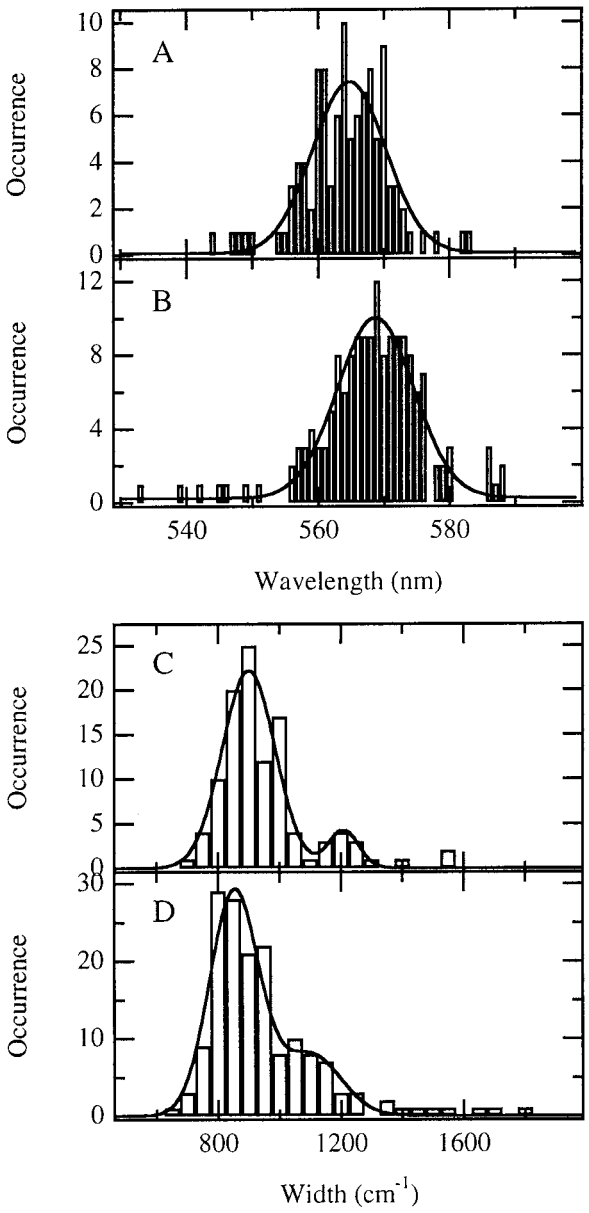

Figure 2. (A) and (B) Histograms of the wavelength of maximum fluorescence emission (1 nm bins) for films characterized immediately after preparation and after drying for a minimum of 12 h at ≈80 °C under vacuum, respectively. Each histogram has been fit with a Gaussian function (solid lines). (C) and (D) Histograms of the widths (50 cm^{-1} bins) of the single-molecule spectra for fresh and dried films, respectively. The solid lines depict fits of these data to two Gaussian functions. The histogram data is offset by half the bin width.

emitted by each molecule prior to photobleaching was measured.[38] Figure 3B,C shows histograms of the data obtained from a large number of molecules in fresh and dried samples. It is clear from these data that the dye molecules entrapped within the dried silicate films emit significantly more total photons than do their fresh-film counterparts. Exponential fits of the histogram data indicate the average photobleaching quantum yields in the fresh and dried samples are approximately $4.7 \pm 0.2 \times 10^{-6}$ and $1.3 \pm 0.1 \times 10^{-6}$, respectively. For these estimates, the fluorescence quantum yield was assumed to be 1.0 and the instrument detection efficiency was taken to be 5%. Data obtained from films dried under vacuum at room temperature fit within this trend.

The fluorescence transients were also used to determine the survival time for each molecule. The survival time was taken

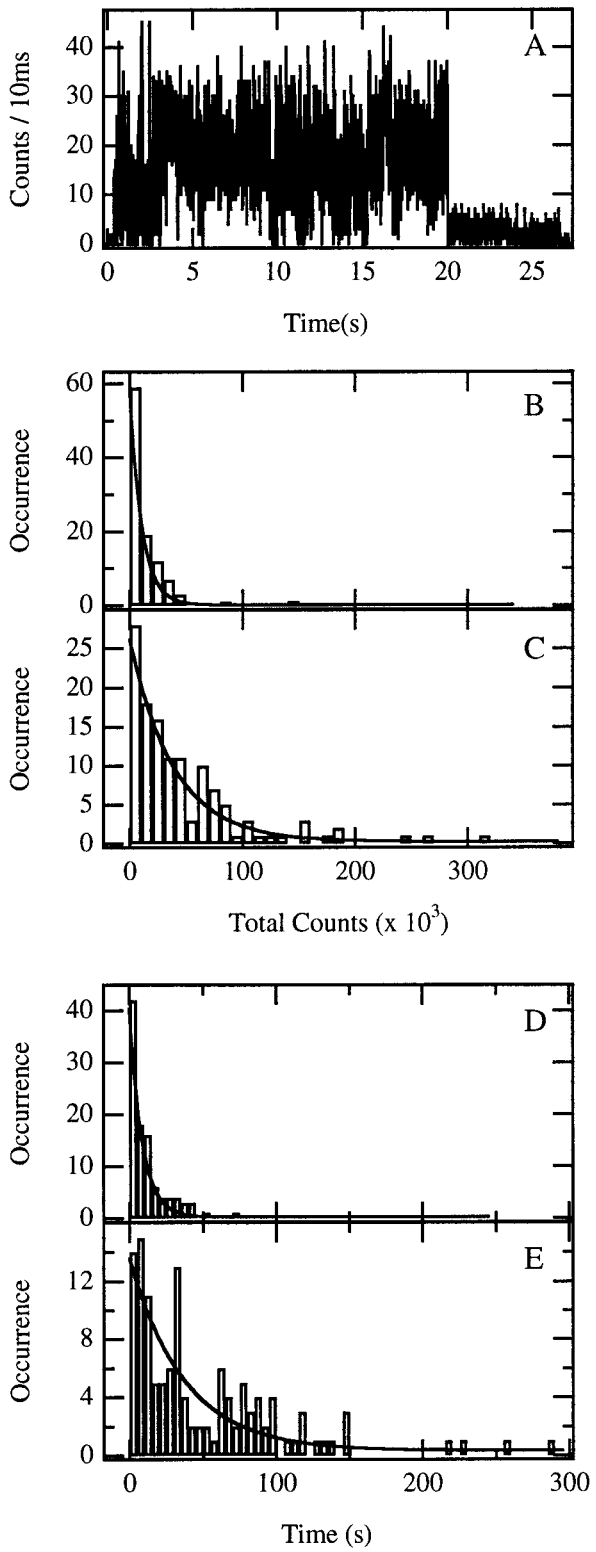

Figure 3. (A) Representative time-dependent trace of the spectrally integrated fluorescence from a single molecule in a film dried at ≈80 °C under vacuum for 12 h. The trace shows signal fluctuations on a variety of time scales. Photodestruction of the molecule occurs near the end of the trace. The time resolution in these data was 10 ms. (B) and (C) Histograms of the total photons emitted by a large number of single molecules in films characterized immediately after preparation and after drying in a vacuum oven (12 h, ≈80 °C), respectively. (D) and (E) Histograms of the survival times for the "fresh" and "dried" films, respectively.

as the total time the molecule survived (before photobleaching) under continuous illumination. The survival times for a number of molecules in both fresh and dried samples are presented in Figure 3D,E in histogram form. Exponential fits of these histograms show an increase in average survival time with drying, giving values of 8.6 ± 0.5 s and 37 ± 6 s, respectively, for the fresh and dried films. Again, data obtained from films dried under intermediate conditions fit within this trend. It should be noted that absolute survival time is highly dependent on excitation efficiency. Without careful determination of the excitation efficiency for each molecule, it is difficult to use this information directly for characterization of individual microenvironmental properties. However, such data can be used to obtain average information and also in conjunction with other measurements (i.e., total emitted photons).

Signal autocorrelations were also calculated from the fluorescence transients.[34,36,37] The autocorrelation function used here has the following form:

$$C(t) = \frac{\langle N(0)N(t)\rangle}{\langle (N(0))^2\rangle}$$

where $N(t)$ represents the fluorescence transient (photon counts) at a particular delay time t. The autocorrelation function is expected to decay from $t = 0$ as a simple exponential.[36] The exponential decay constant is a measure of the signal fluctuation rate for the single molecule. The dependence of the fluctuation rate on film-drying conditions is of particular interest here.

Figure 4A,B presents an example of the time-dependent data utilized and its corresponding autocorrelation. Only molecules surviving longer than 5 s were analyzed. The autocorrelations often showed significant deviation from exponential behavior on long time scales (i.e., >2 s, as shown in Figure 4B). Such deviations are due to the relatively few (statistically insignificant) signal transitions observed on these longer time scales.[37] To avoid errors associated with inclusion of such data, only the initial 10% of each autocorrelation was fit. In addition, the decays could only be fit with biexponential functions. The fastest component of the biexponential fits usually gave a time constant smaller than the time resolution. These data are not used; only data showing correlation times attributable to blinking on longer time scales are reported. Histograms of these data for the fresh and dried silicate films are shown in Figure 4C,D. Clearly, the dopant molecules in the dried films show much shorter correlation times, indicating the signal fluctuation rate is greater than in the fresh films. Fits of the histogram data yield average correlation times of 3.2 ± 0.6 s and 0.81 ± 0.04 s for the fresh and dried samples, respectively. These results are consistent with the qualitative observation that more fluctuations are observed in the fluorescence from molecules in the dried films.

Information on the signal fluctuation mechanism was obtained by recording fluorescence transients for individual molecules at a series of incident powers. For the vast majority of molecules studied, the autocorrelations derived from these transients were power dependent. The signal correlation times (longer time scale fluctuations) obtained by fitting the autocorrelations showed a monotonic decrease with increasing power. These results prove the fluctuations are photoinduced, resulting from excitation of the molecule.[34,35]

In addition to the single-molecule studies presented above, FTIR spectroscopy was also used to examine the physical structure of the silicate films dried under different conditions. These studies provide information on the average properties of the films. Spectra obtained for fresh (a few minutes after spin casting) and oven-dried films cast onto silicon wafers (but otherwise similar to those used in the single-molecule studies)

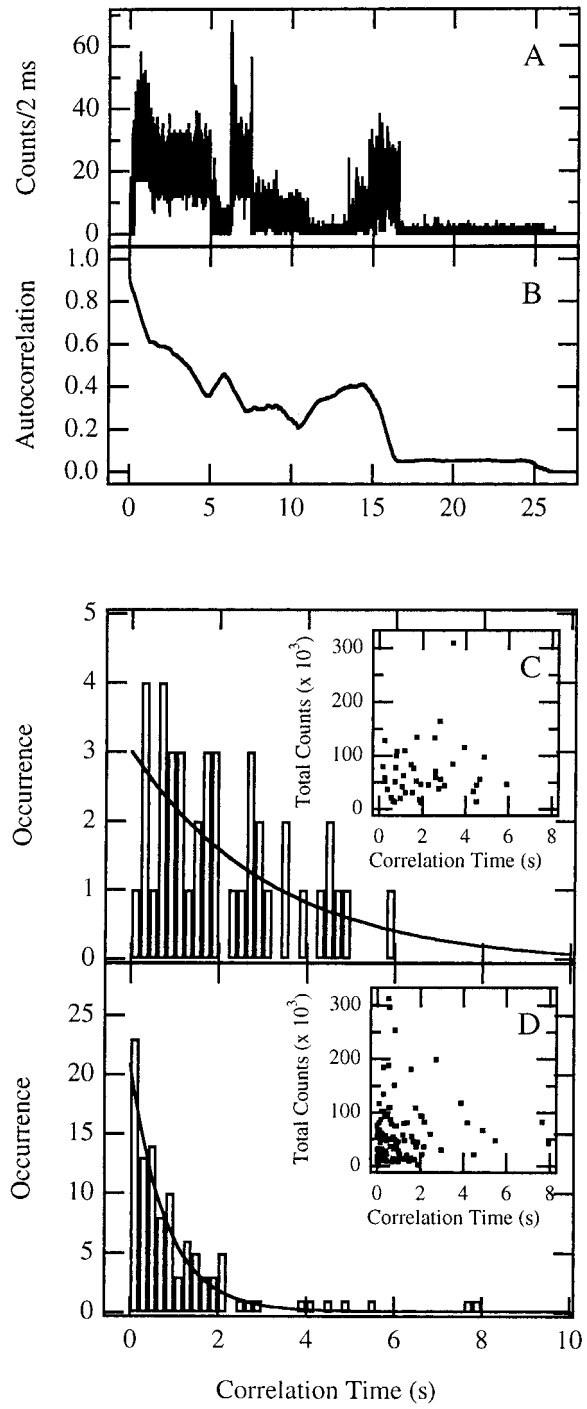

Figure 4. (A) Time dependence of the spectrally integrated fluorescence from a single molecule in a vacuum-oven dried film. The time resolution is 2 ms. (B) Autocorrelation of the data in (A). The initial 10% (at most) of similar traces for all single molecules were fit to double exponential functions. (C) Histogram of the correlation times (the inverse of the longer of the two decay constants) observed for single molecules in a fresh silicate film. (B) Histograms of the correlation times for single molecules in the vacuum-dried films (12 h, ≈80 °C). Single-exponential fits of these histograms yield correlation times of 3.2 ± 0.6 s and 0.81 ± 0.04 s for the fresh and dried samples, respectively. The insets in (C) and (D) show the relationship between correlation time and total photons emitted.

are shown in Figure 5. Three bands characteristic of the Si−O bond vibrations are observed at 1070, 800, and 440 cm^{-1}. The former two bands can be attributed to the asymmetric and symmetric stretching vibrations of Si−O−Si whereas the latter is assigned to an Si−O−Si bend. In addition to these vibrations,

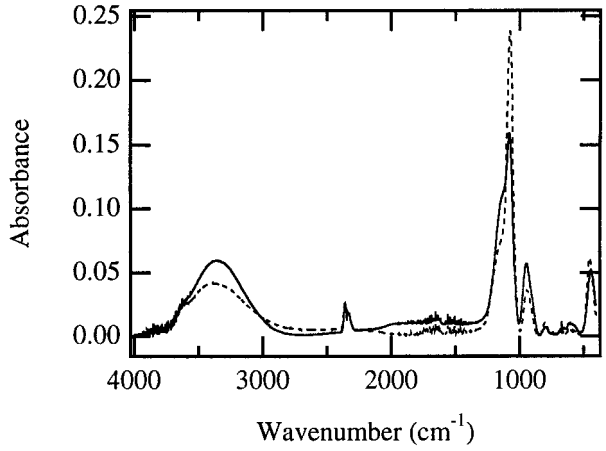

Figure 5. FTIR spectra for fresh (−) and dried (- - -) silicate thin films spin cast onto silicon substrates. The OH stretching vibration appears as a broad band near 3300 cm^{-1}. The Si−OH stretch occurs near 940 cm^{-1}. The Si−O−Si stretching vibrations appear at 1070 and 800 cm^{-1}, while the Si−O−Si bend occurs at 440 cm^{-1}. The peaks at 2360 cm^{-1} are due to atmospheric CO_2.

a broad absorption band near 3300 cm^{-1}, attributed to the OH stretching vibration, and a small band near 940 cm^{-1}, attributed to Si−OH stretching, are also observed. As is readily apparent in these spectra, the broad band at 3300 cm^{-1} and the band at 940 cm^{-1} (Si−OH) decrease in intensity with drying whereas the bands at 1070, 800, and 440 cm^{-1} (Si−O−Si) increase. These changes reflect an increase in the degree of cross-linking in the dried films.

IV. Discussion

The spectroscopic data presented in Figure 2 provide important information on the microscopic polarity and heterogeneity of silicate films, as a function of drying conditions. In many respects, the results obtained complement those from bulk spectroscopic investigations.[6,7,39,40] However, single-molecule studies yield much more detailed information on the distribution of microenvironments found in these films. Figure 2 shows that RhB fluorescence from the dried films is, on average, red shifted by about 4 nm from that of the fresh films. The relatively small spectral shift suggests that the microenvironments in these films are chemically quite similar. However, because RhB fluorescence shifts to the red in more polar environments,[41] it may be concluded that the local environments in the dried silicates are (on average) somewhat more polar than in the fresh samples. This result is consistent with bulk spectroscopic measurements that show a red shifting of the fluorescence from different dyes (reflecting an increase in film polarity) as the gel dries.[7,18,42−44]

The increase in film polarity with drying can be attributed to the evaporation of residual solvent, and to changes in the polarity of the silica cage surrounding the entrapped dye molecule. As the film is heated, methanol and water are removed from the pores and additional condensation occurs, causing the pores to collapse around the dopant. These changes are reflected in the FTIR spectra of the fresh and dried films (see Figure 5), which show a reduction in the broad solvent band at 3300 cm^{-1} with heating. The spectra also show a reduction in the Si−OH stretching band at 940 cm^{-1} and a corresponding increase in the Si−O−Si stretching vibration at 1070 cm^{-1} for the dried film. The microenvironment surrounding the entrapped dye thus changes from a mostly methanolic environment (fresh film) to one that is largely silica comprised of Si−OH and Si−O−Si functionalities and adsorbed water (dried film). More polar

microenvironments result. It is also possible that as the residual solvent evaporates and the pores collapse, the dye molecules interact more strongly with surface silanol groups,[15] possibly via the formation of hydrogen bonds.[42] Such interactions likely contribute to the red shift in the fluorescence spectrum.

Figure 2 also shows the existence of a very broad distribution of molecular scale environments in the silicate films. As shown previously, these materials are much more heterogeneous than common organic polymer films.[31] Variations in the local polarity of the individual microenvironments may arise from microscopic differences in solvent content and in the degree of hydrolysis and condensation in the silicate network surrounding a given probe molecule. Differences between the fresh and dried films are therefore also reflected in the relative widths of their fluorescence distributions (see Figure 2A,B). The fwhm of these distributions for fresh and dried samples are again 13 ± 1 nm and 14 ± 1 nm, respectively. While the difference is small, the increased breadth of the dried-film distribution is consistent with increased material heterogeneity (i.e., a greater range of microenvironmental polarities). The most notable contributors to the increased width are the several molecules that emit near the blue and red edges of the dried film distribution (see Figure 2). While the exact chemical compositions of such environments cannot be determined, it is clear that some of these environments are as nonpolar as those found in the fresh film, while others are significantly more polar. The nonpolar environments may be due to the presence of unhydrolyzed methoxy groups on the silicate pore surfaces, whereas the more polar environments may result from further hydrolysis and pore collapse. Regardless of their specific chemical origins, the observed increase in film heterogeneity can be expected to result in increased variability in the stability/reactivity of dopant molecules (see below).

The spectral width data shown in Figure 2C,D provides additional information on the silicate microenvironments that is not readily obtained from bulk spectroscopic data. Notably, two Gaussian functions were required to properly fit the histogram data, implying that two distinct classes of environment exist within these films. The positions of these distributions provide a means for classifying the polarity and rigidity of the microenvironments. From continuum models for solvent-dependent charge-transfer transitions, red-shifted spectra from more polar environments are expected to be somewhat broadened,[45] although in more rigid materials such as those studied here, narrower spectra may also be obtained.[46,47] The width distributions reflect this complexity. As has been shown recently, the activity of various intramolecular vibrational motions may also depend on the local environment.[37] Molecules entrapped in rigid microenvironments may yield narrower spectra via the "freezing out" of certain molecular motions. Therefore, the slight shift to smaller widths for both distributions (47 ± 8 cm^{-1} and 100 ± 35 cm^{-1}) as the samples are dried reflect increased microenvironmental rigidity.[47] The two distinct distributions observed most likely arise from the presence of environments differing primarily in their rigidity.[47]

While the single-molecule spectral data point to differences in material polarity and heterogeneity, the fluorescence transients also provide information not readily available from bulk spectroscopic studies. The time-dependent single-molecule emission characteristics (i.e. blinking behaviors) observed here are dramatically different for molecules in films dried under different conditions. Single-molecule blinking on the millisecond time scale often arises from intersystem crossing of the excited dye to a nonemissive triplet state of relatively long lifetime.[35] The power-dependence of the autocorrelation functions measured here is consistent with the participation of a triplet state in the observed signal fluctuations (i.e., "triplet blinking"). Higher incident powers lead to more rapid excitation of the dye, and hence, an increased rate of triplet formation. As a result, the fluorescence blinks off more frequently in time and the signal correlation time is reduced, as observed. As triplet blinking likely makes a substantial contribution to the observed fluctuations, information on the rate of triplet state formation and its lifetime can be obtained. In addition, the fluorescence transients yield the total number of photons emitted by each molecule (prior to bleaching), and the survival time of each molecule (under continuous illumination). The results of these experiments are particularly important, representing a new means for characterizing heterogeneity in film microenvironmental properties (i.e., rigidity and dopant mobility). Such measurements may also provide new information on the effects of dopant surface adsorption.[42,43,48]

The results in Figure 3 indicate that the total number of photons emitted (on average) by a single molecule is nearly a factor of 4 (3.7 ± 0.6) greater in the dried films than in the fresh. In addition, they also show the average survival time of the molecules in the dried film is about four (4.3 ± 0.7) times larger than in the fresh films. Possible explanations for the increase in total emitted photons include (i) an increase in the fluorescence quantum yield of the dye and/or (ii) an increase in dye stability, as manifested by a reduction in the rate of photobleaching.

The increase in total number of photons emitted cannot be explained entirely by an increase in quantum yield, which has been reported as 0.49 and 0.71 for the acid and base forms of RhB, respectively, in ethanol solution.[49] It is expected to be even higher in the silicate matrix, due to the restriction of molecular motions participating in nonradiative relaxation of the singlet excited state. Previously published results indeed show an increase in the excited-state lifetime (relative to solution)[50] for RhB[40] and other dyes entrapped within silicate materials.[16,51,52] In addition, if the increase in total photons was due solely to an increase in fluorescence quantum yield, the average survival times would be similar for the fresh and dried samples (assuming similar absorption cross sections, intersystem crossing rates, etc.). Again, they differ by a factor of 4. Therefore, it is highly unlikely that the 4-fold increase in total photons results from a corresponding 4-fold increase in quantum yield. In fact, the similar increase in total photons and survival time is consistent with little or no change in quantum yield. It is therefore concluded that these increases result primarily from an increase in dye stability. Indeed, recent bulk spectroscopic studies have shown many dyes to be more stable (relative to solution) when entrapped within silicates.[14,40,51]

The irreversible photobleaching of RhB is believed to occur via reaction of the dye with singlet oxygen generated during the quenching of the excited triplet state.[53] Therefore, molecules that cross more frequently to a longer-lived triplet state have a greater probability for reaction with oxygen and are chemically less stable. Increased dye stability observed in the dried films may then result from (i) a decrease in the intersystem crossing rate, (ii) a decrease in the triplet lifetime, (iii) a reduction in the oxygen permeability/mobility,[13] or (iv) a reduction in certain dye motions required for photobleaching.

Based on the results of the autocorrelation analysis (Figure 4), it is not likely that the observed increase in dye stability results from either of the first two possibilities. The results clearly show that shorter correlation times (by a factor of 4) are observed for the dye molecules entrapped in the dried films,

reflecting an increase in the rate of signal fluctuations (blinking). Such results are consistent with an increase (rather than a decrease) in the intersystem crossing rate. The observed decrease in average correlation time for the dried samples is also consistent with a decrease in triplet lifetime.[36] However, it is believed that the increased rate of signal fluctuations observed for the dried films actually reflects an increase (rather than a decrease) in the triplet lifetime. Such would be the case were the time resolution in the experiment not sufficient to faithfully reproduce the fastest signal fluctuations. It has been reported that triplet lifetimes of other dyes indeed become longer in silicate matrixes.[16,54] An increase in dark-state lifetime would then result in an increase in the number of fluctuations observed, and hence, a decrease in the correlation time. Since the triplet lifetime of RhB in solution is very short (1.6 μs)[55] and the time resolution for the data shown in Figure 4 is 2 ms, it is believed this latter effect contributes most significantly. Experiments performed with 500 μs resolution (instrument limited) show a similar reduction in the correlation time for the dried film data, suggesting the true triplet lifetime is too short to accurately measure here.

As shown in the insets of Figure 4C,D, there exists an apparent relationship between the correlation time and total photons emitted by a given molecule. In general, molecules exhibiting more signal fluctuations are observed to survive longer. Since a large number of factors contribute to variations in the data, this correlation is not particularly strong. Ignoring other factors, the longer triplet lifetime and greater triplet formation rate (i.e., more fluctuations) deduced above would normally lead to reduced dye stability. Since it is observed that molecules that cross more frequently to a longer-lived triplet state are also more stable, it may be concluded that increased dopant stability must result from reduced dye and/or oxygen mobility in the dried films. As shown recently by Liu et al.,[54] oxygen permeability in silicate films is highly dependent on material preparation conditions. The reduction in reactant mobility is attributable to an increase in the density and rigidity of the silicate network in the dried films, as supported by the single-molecule data and the FTIR data presented above. Reduced dye mobility may also arise from adsorption of the dye to surface sites within the silicate,[42,43,48] as is likely indicated by the red shift in the dried-film fluorescence spectra.

Because the single-molecule methods employed here provide information on the properties of individual molecular environments, conclusions about the distribution of dye stabilities may also be drawn. While the average molecule exhibits a 4-fold increase in stability in the dry sample, numerous molecules are observed to last from 5 to 10 times longer than the vast majority of molecules in the fresh sample. This observation suggests that the improvement in dye stability may indeed be much greater in some local microenvironments. Such molecules may be entrapped in particularly isolated environments that are far less accessible to oxygen, or they may be adsorbed more strongly to the silicate walls. A better understanding of the chemical composition of such environments may allow for films with dramatically improved dopant stability to be prepared in the future.

As a final caveat to the above discussion, it should be noted that signal fluctuations may result from a number of processes. For example, spectral diffusion may be an important contributor.[32,33] The extent to which spectral diffusion contributes to the fluctuations is presently being investigated. For these experiments, single-molecule fluorescence spectra are acquired with 0.5 s time resolution. Large jumps (greater than 30 nm) in emission maxima are infrequently observed for a small fraction ($\approx$13%) of dopant molecules. To further assess the dependence of the fluctuations on shifts in the excitation spectrum, two different excitation wavelengths have been employed (i.e., 514.5 and 543.5 nm) in the recording of fluorescence transients. The data sets collected for fresh and dried samples using these two wavelengths showed identical trends, with the dried film data showing shorter correlation times in both cases. Therefore, it is concluded that spectral diffusion is not the dominant contributor to the observed fluctuations.

V. Conclusions

Single-molecule spectroscopic studies of sol−gel-derived silicate films have been used to obtain valuable information on the variations in microenvironmental properties within single films, as well as between films prepared under different drying conditions. In this work, single-molecule fluorescence spectra were used to show that the microenvironments in rigorously dried films are slightly more polar and more rigid than their fresh counterparts and incorporate a broader range of microenvironments having different properties. Detailed analyses of the time-dependent emission characteristics of single molecules (fluorescence transients) were used to show that RhB molecules entrapped within the dried films are approximately four times more stable than their fresh-film counterparts. The transients also showed that the intersystem crossing rate and/or triplet lifetime are also greater in the dried films. Because of the role played by oxygen in the photochemical bleaching of RhB, these results likely reflect a decrease in oxygen mobility within the dried films, and/or a reduction in the translational/rotational mobility of the entrapped dye. The apparent reduction in dye and/or oxygen mobility was attributed to an increase in the extent of silicate cross-linking, evaporation of entrapped solvent, and increased adsorption of the dye to the silicate pore surfaces as the films were dried. Increased film density and rigidity was reflected in both the single-molecule and FTIR spectroscopic data. These studies have provided a better understanding of the types of microenvironments present in silicate films prepared and dried under different conditions. In the future, such studies will allow for fabrication of materials with improved physical and chemical properties and superior performance.

Acknowledgment. The authors gratefully acknowledge the support of the Army Research Office (via the Defense EPSCoR Program) and Kansas State University in these studies. D.A.H. also thanks 3M Corporation for additional financial support. M.M.C. acknowledges additional support from the Office of Naval Research. Stephanie Rasinski and Hanming Wang are thanked for their contributions to the early phases of this project.

References and Notes

(1) Brinker, J.; Scherer, G. *Sol−Gel Science*; Academic Press: New York, 1989.

(2) Lev. O.; Tsionsky, M.; Rabinovich, L.; Glezer, V.; Sampath, S.; Pankratov, I.; Gun, J. *Anal. Chem.* **1995**, *67*, 22A.

(3) Avnir, D. *Acc. Chem. Res.* **1995**, *28*, 328.

(4) Collinson, M. M. *Mikrochim. Acta* **1998**, *129*, 149.

(5) Avnir, D.; Klein, L. C.; Levy, D.; Schubert, U.; Wojcik, A. B. In *The Chemistry of Organic Silicon Compounds*, Vol. 2; 1998; Chapter 40, pp 2317−2362.

(6) Dunn, B.; Zink, J. I. *J. Mater. Chem.* **1991**, *1*, 903.

(7) Dunn, B.; Zink, J. I. *Chem. Mater.* **1997**, *9*, 2280.

(8) Dave, B. C.; Dunn, B.; Valentine, J. S.; Zink, J. I. *Anal. Chem.* **1994**, *66*, 1120A.

(9) Lin, J.; Brown, C. W. *Trends Anal. Chem.* **1997**, *14*, 200.

(10) Gvishi, R.; Narang, U.; Ruland, G.; Kumar, D. N.; Prasad, P. N. *Appl. Organometallic Chem.* **1997**, *11*, 107.

(11) Levy, D. *Chem. Mater*. **1997**, *9*, 2666.
(12) Dunn, B.; Farrington, G. C.; Katz, B. *Solid State Ionics* **1994**, *70/71*, 3.
(13) Samuel, J.; Polevaya, Y.; Ottolenghi, M.; Avnir, D. *Chem. Mater*. **1994**, *6*, 1457.
(14) Avnir, D.; Levy, D.; Reisfeld, R. *J. Phys. Chem.* **1984**, *88*, 5956.
(15) Matsui, K.; Momose, F. *Chem. Mater.* **1997**, *9*, 2588.
(16) Innocenzi, P.; Kozuka, H.; Yoko, T. *J. Phys. Chem. B* **1997**, *101*, 2285.
(17) Collinson, M. M.; Zambrano, P.; Wang, H.; Taussig, J. *Langmuir* **1999**, *15*, 662.
(18) Matsui, K.; Nozawa, K. *Bull. Chem. Soc. Jpn.* **1997**, *70*, 2331.
(19) Kaufman, V. R.; Avnir, D. *Langmuir* **1986**, *2*, 717.
(20) Nishikiori, H.; Fujii, T. *J. Phys. Chem.* **1997**, *101*, 3680.
(21) Dunbar, R. A.; Jordan, J. D.; Bright, F. V. *Anal. Chem.* **1996**, *68*, 604.
(22) Diaz, A. N.; Lovillo, J.; Peinado, M. C. R. *Chem. Mater*. **1997**, *9*, 2647.
(23) Narang, U.; Wang, R.; Prasad, P. N.; Bright, F. V. *J. Phys. Chem.* **1994**, *98*, 17.
(24) Narang, U.; Jordan, J. D.; Bright, F. V.; Prasad, P. N. *J. Phys. Chem.* **1994**, *98*, 8101.
(25) Sieminska, L.; Zerda, T. W. *J. Phys. Chem*. **1996**, *100*, 4591.
(26) Gvishi, R.; Narang, U.; Bright, F. V.; Prasad, P. N. *Chem. Mater*. **1995**, *7*, 1703.
(27) Betzig, E.; Chichester, R. J. *Science* **1993**, *262*, 1422.
(28) Xie, X. S. *Acc. Chem. Res.* **1996**, *29*, 598.
(29) Moerner, W. E.; Kador, L. *Phys. Rev. Lett.* **1989**, *62*, 2535.
(30) Moerner, W. E. *Acc. Chem. Res.* **1996**, *29*, 563.
(31) Wang, H.; Bardo, A. M.; Collinson, M. M.; Higgins, D. A. *J. Phys. Chem. B* **1998**, *102*, 7231.
(32) Ambrose, W. P.; Moerner, W. E. *Nature* **1991**, *349*, 225.
(33) Lu, H. P.; Xie, X. S. *Nature* **1997**, *385*, 143.
(34) Dickson, R. M.; Cubitt, A. B.; Tsien, R. Y.; Moerner, W. E. *Nature* **1997**, *388*, 355.
(35) Ha, T.; Enderle, T.; Chemla, D. S.; Selvin, P. R.; Weiss, S. *Chem. Phys. Lett.* **1997**, *271*, 1.
(36) Yip, W.-T.; Hu, D.; Yu, J.; Vanden Bout, D. A.; Barbara, P. F. *J. Phys. Chem. A* **1998**, *102*, 7564.
(37) Weston, K. D.; Carson, P. J.; Metiu, H.; Buratto, S. K. *J. Chem. Phys.* **1998**, *109*, 7474.
(38) Wennmalm, S.; Rigler, R. *J. Phys. Chem. B* **1999**, *103*, 2516.
(39) McKiernan, J.; Pouxviel, J.-C.; Dunn, B.; Zink, J. I. *J. Phys. Chem.* **1989**, *93*, 2129.
(40) Negishi, N.; Fujino, M.; Yamashita, H.; Fox, M. A.; Anpo, M. *Langmuir* **1994**, *10*, 1772.
(41) Snare, M. J.; Trelor, F. E.; Ghiggio, K. P.; Thistlethwaite, P. J. *J. Photochem. 18* **1982**, 335.
(42) Matsui, K.; Matsuzuka, T.; Fujita, H. *J. Phys. Chem.* **1989**, *93*, 4991.
(43) Suratwala, T.; Gardlund, Z.; Davidson, K.; Uhlmann, D. R.; Watson, J.; Peyghambarian, N. *Chem. Mater*. **1998**, *10*, 190.
(44) Innocenzi, P.; Kozuka, H.; Yoko, T. *J. Non-Cryst. Solids* **1996**, *201*, 26.
(45) Brunschwig, B. S.; Ehrenson, S.; Sutin, N. *J. Phys. Chem.* **1987**, *91*, 4714.
(46) Marcus, R. A. *J. Phys. Chem.* **1990**, *94*, 4963.
(47) Hou, Y.; Bardo, A. M.; Martinez, C.; Higgins, D. A. *J. Phys. Chem. B* **2000**, *104*, 212.
(48) Huang, M. H.; Soyez, H. M.; Dunn, B. S.; Zink, J. I. *Chem. Mater*. **2000**, *12*, 231.
(49) Ferguson, J.; Mau, A. W.-H. *Aust. J. Chem.* **1973**, *26*, 1617.
(50) Sadkowski, P. J.; Fleming, G. R. *Chem. Phys. Lett.* **1978**, *57*, 526.
(51) Avnir, D.; Kaufman, V. R.; Reisfeld, R. *J. Non-Cryst. Solids* **1985**, *74*, 395.
(52) Levy, D.; Ocaña, M.; Serna, C. J. *Langmuir* **1994**, *10*, 2683.
(53) Gollnick, K.; Franken, T.; Fouda, M. F. R. *Tetrahedron Lett.* **1981**, *22*, 4049.
(54) Liu, H.-Y.; Switalski, S. C.; Coltrain, B. K.; Merkel, P. B. *Appl. Spectrosc.* **1992**, *46*, 1266.
(55) Korobov, V. E.; Shubin, V. V.; Chibisov, A. K. *Chem. Phys. Lett.* **1977**, *45*, 498.